Biophysical Journal, Volume 97

Supporting Material

Coupling of S4 helix Translocation and S6 Gating Analyzed by Molecular Dynamic Simulations of Mutated Kv channels

Manami Nishizawa and Kazuhisa Nishizawa

Supplementary Text and Figures:

Supplementary Text

1.

The initial bilayer membrane of 434 DPPC molecules (217 molecules for each of outer and inner leaflet) was generated by duplicating the bilayer used previously (40) and subjected it to a 2ns equilibration run. The chimeric channel was placed such that the lipid molecules contained in the X-ray crystal are approximately in line with the DPPC bilayer (Fig.1). In this position the center of mass of the channel protein is 1.1Å above that the center of mass of the lipid membrane. 172 DPPC molecules (86 molecules for each leaflet) overlapping with the channel were removed. The peptide/DPPC system was hydrated with 12500 water molecules containing 7 sodium and 11 chloride ions. Prior to the productive runs, a 2ns equilibration run was done with harmonic restraints on all peptide atoms. For this study side-chain ionization states were set at the default ionization pattern for all residues. All histidine residues were set at neutral.

For all simulations in this study, the bond lengths were constrained using LINCS (41). The cutoff for the Lennard-Jones interactions was set at 9 Å. To account for the long-range electrostatic interactions under the periodic boundary condition, the Particle-Mesh Ewald (PME) algorithm (42) was used with the real-space cutoff at 9Å and the maximal grid size of 0.12 Å. The integration time-step was set at 2.5fs. The temperature was set at 323K with Berendsen coupling (43). The pressure was controlled by the Berendsen barostat at 1 atm with the independent (semi-isotropic) coupling in the x,y- and z-directions.

2. (**Comment on Internal motions of S6**)

For the two-fold symmetry-like narrowing, two S6 helices exhibiting narrowing movement showed deviation toward the central axis not only by the VIV segment, but also by a wider segment of S6 involving several residues upstream (e.g., E395W-Eo-S4$_{middle}$, E395W-F401A-F402A-S4$_{low}$). Thus, the S6 conformational change upon closure involves hinge-like bending at a fairly high position, although, for some simulations, the manner in which each of the residues moved was markedly different among subunits (e.g., E395W-F401A-F402A-V478W-Eo-S4$_{middle}$, E395W-E+-S4$_{middle}$ and E395W-F401A-F402A-S4$_{middle}$.).

3. (**Implications for short-lived closed states, Cf and Ci.)**

Unlike Kv2.1, clear sub-conductance levels have not been reported to our knowledge for wild-type *Shaker* or Kv1.2 channel of mammals. On the other hand, it closes briefly into short-lived closed states. Single channel analysis of *Shaker* by Hoshi et al (67) has shown that, in addition to the resting closed states within the activation-path, there are at least two closed states, Cf and Ci, which are not in the activation-path. (See also Figure 10A of ref.23). Although we cannot rule out the possibility that Ci reflects a special state of selectivity filter, such interpretation does not provide a simple model because Cf and Ci appear to be an intermediate state that links the classical closed state to the open state (23). It is therefore tempting to envisage that, while the closed state with four-fold symmetry may correspond to the stable closure, some heteromeric pore conformations observed in our simulations may correspond to short-lived closed states such as Ci or Cfs.

4. (**A detailed version of the legend for Fig.1)**

(A) The view from the bottom (left) and from the side (right) of the initial configuration for the wt-chimera channel with $S4_{high}$–settings are shown. Blue, green, ochre and red ribbons show subunit-1, -2, -3 and -4, respectively. For clarity, loops between helices are hidden. For the side view (right), subunit-4 (red ribbons) is also hidden. The side view represents the view from the position of subunit-4 and, to improve clarity, the water (gray lines) and DPPC molecules located outside of the ~1.8nm-thick slice containing subunit-1 and –3 are not shown. DPPC molecules representation: light blue lines for acyl chains and ochre, red and blue lines for phosphorus, oxygen and nitrogen atoms, respectively. (B)The initial conformation for wt-chimera-$S4_{high}$, -$S4_{middle}$ and –$S4_{low}$. Only subunit-1 (blue) is shown, along with S5 and S6 of the adjacent subunit-2 (green). The residues introduced for a mutation are highlighted by Van del Waals representation (F401 and F402) and licorice representation (E395). I372 L382 and L385,are shown in pink licorice which interact with F401 and F402 creating a hydrophobic cluster between S4 and the adjacent subunit S5. For the gating-charge-carrying residues (R2, R3, R4 and K5), the C_α is shown as a yellow ball and the sidechain as silver licorice.

5. **(A detailed version of the legend for Fig.5)**

Effect of perturbation of one subunit on the location of the S4-S5 linker, S5 and S6. Shown are the results for the simulation in which only S4 of blue subunit (subunit 1) (left column) or S5 of yellow subunit (subunit 3) (right column) was pulled down, respectively. Otherwise, the initial configuration/conformation was the same as the

wt-chimera-E+-$S4_{high}$. Four subunits are shown with the same coloring scheme as in the graphical images of Fig.3. (A) The distance of V478 from the central axis of the pore domain. (B) The distance of the com of S4-S5 linker from the central axis. (C) z-position (i.e., vertical position) of the com of S4-S5 linker. (D) The z-position of the com of S5. (E) Rotational angle (in degrees) around the central axis. A positive value indicates clockwise rotation when viewed from the intracellular side.

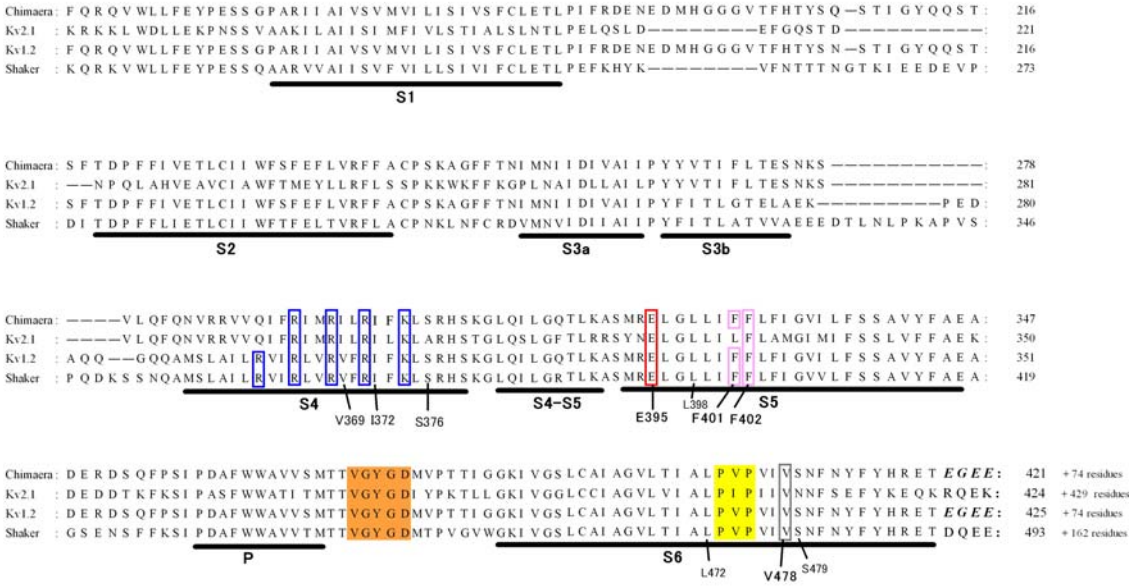

Fig.S1 Sequence alignment of the Kv1.2-Kv2.1 chimera channel, rat Kv2.1 (GI, 24418849; Swiss-Prot entry No. P15387), rat Kv1.2 (GI, 1235594; P63142) and Drosophila melanogaster Shaker Kv (GI, 13432103; P08510). The alignment was basically the same as the one shown in (Long et al 2007), but four residues (EGEE) on the COOH-terminus side are included. Residues discussed in the text are highlighted with blue boxes (gating-charge-carrying Arg and Lys), a red box (E395), pink boxes (F401 and F402), an orange shade (VGYGD motif of selectivity filter), a yellow shade (PVP motif) and a gray box (V478). Secondary structure elements are indicated with bars under the sequences. V369, I372 and S376, which are substituted in the ILT mutant (see text), are highlighted. At the COOH-terminus the number of deleted amino acid residues is shown based on the Swiss-Prot data. Note that the N-terminus has additional residues: 144 for Kv1.2, 170 for Kv2.1 and 208 for Shaker.

Reference for Fig.S1

Long, S.B., X. Tao, E.B. Campbell and R. MacKinnon. .2007. Atomic structure of s voltage-dependent K+ channel in a lipid membrane-like environment. Nature 450: 376-382

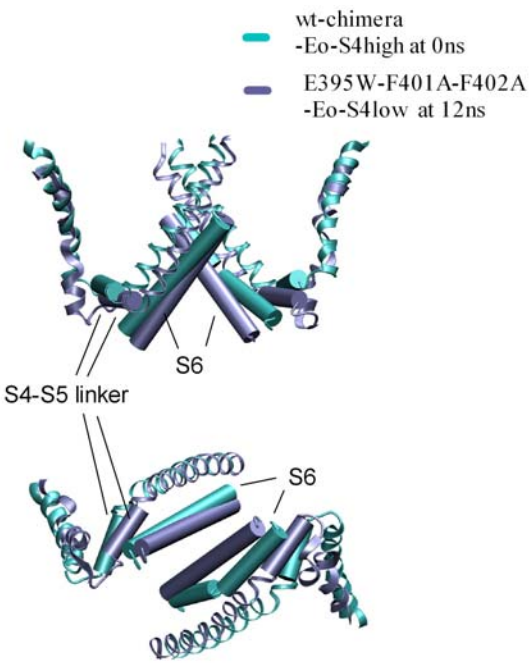

Fig.S2 Translocation of the S4-S5 linker, S5 and S6 in the simulation E395W-F401A-F402A-Eo-S4low. Shown is a representative snapshot of S4-S5 linker, S5 and S6 at the 0ns (gray cylinder) and 12ns (blue cylinder), which exhibited a S6 narrowing movement in a two-fold symmetry-like structure.

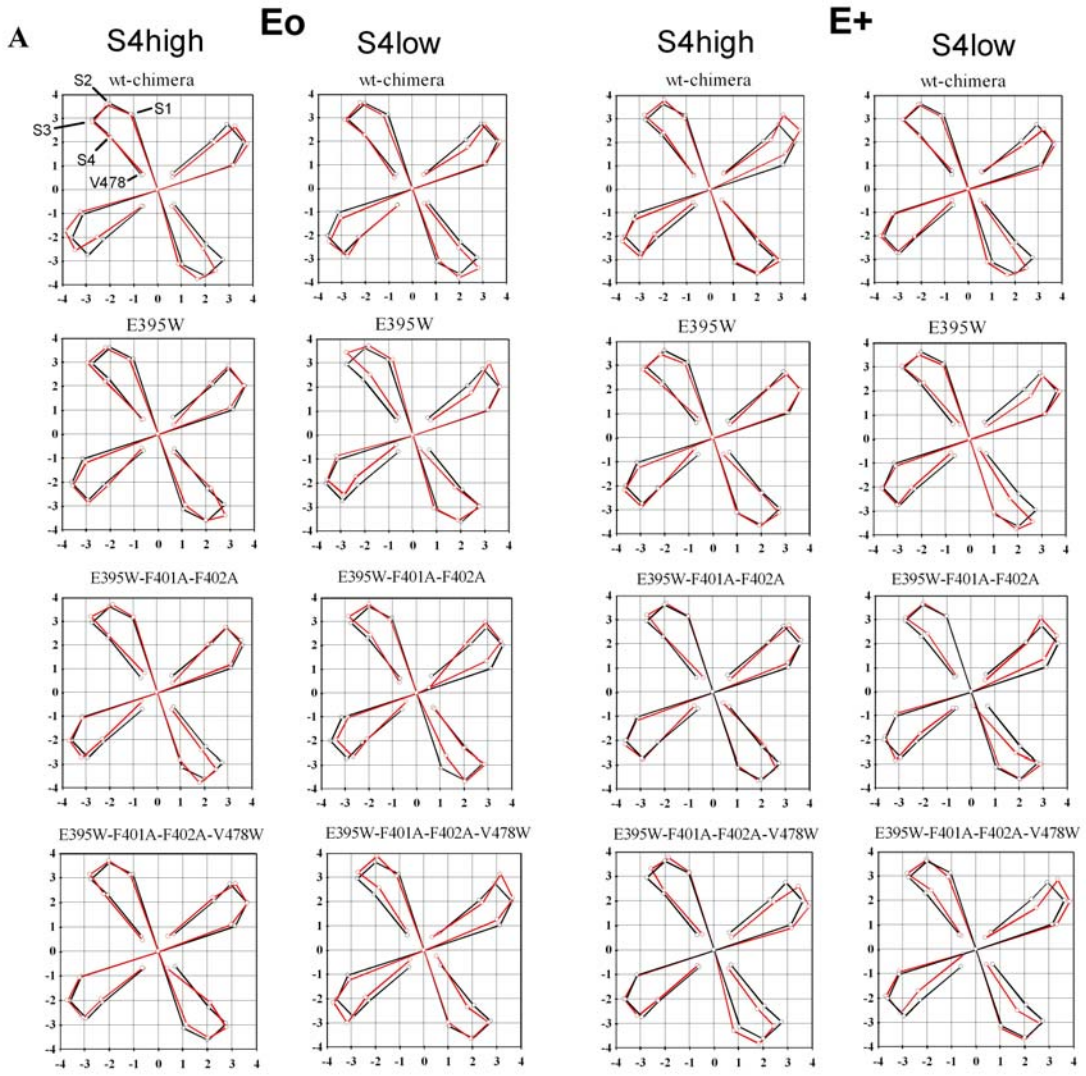

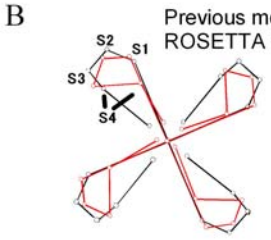

Fig.S3 Movement of the center of mass (com) of S1, S2, S3 and S4 and the Cα of V478.
(A) Results for the simulations with S4high and S4low.
Conformations at 0ns and 12ns are represented by black and red lines, respectively, which connect the coms of S1-S4. Shown is the view from the extracellular side.
(B) Prediction based on the recent model of Shaker by Pathak et al.(2007).
Black and red lines represent the open and closed states, respectively.

Reference for Fig.S2

Pathak, M. M., V. Yarov-Yarovoy, G. .Agarwal, B. Roux, P. Barth, S. Kohout, F. Tombola and E. Y. Isacoff. 2007.
Closing in on the resting state of the Shaker K+ channel. Neuron. 56: 124-140.

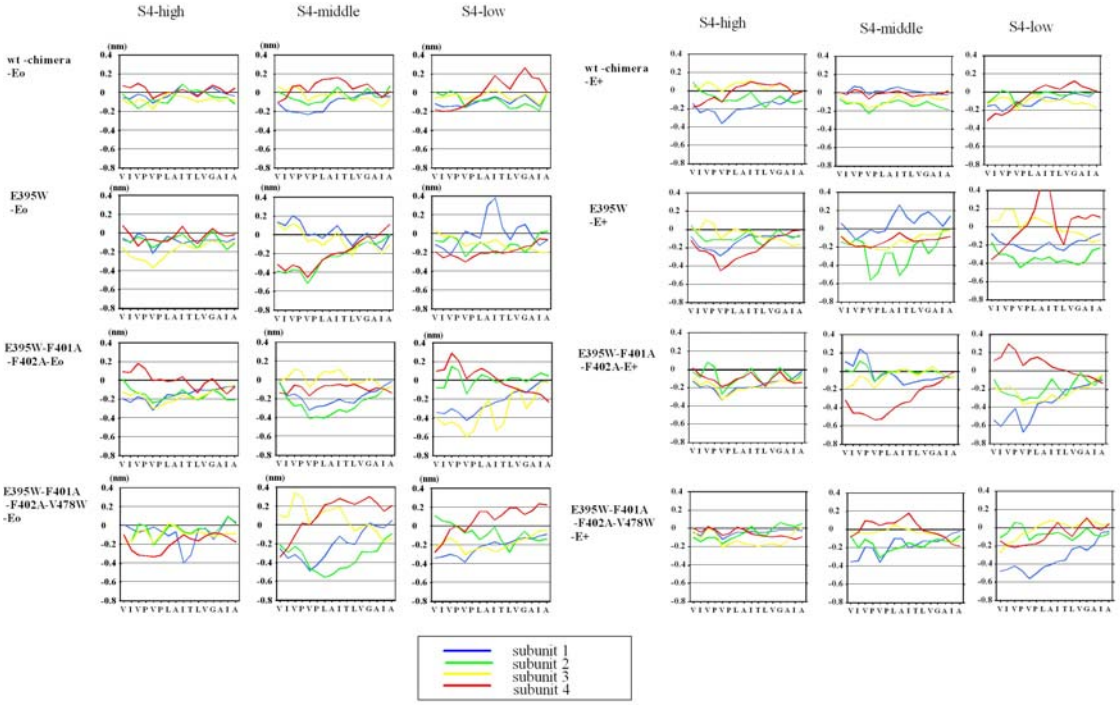

Fig.S4 Internal motions of S6.
Change in the distance of each residue from the central axis of the pore domain, relative to the value in the initial conformation. For example, a negative value mean that the residue moved toward the central axis.

Technical details for the umbrella sampling

The Gromacs suit was used for the umbrella sampling.
The average z-position of the four Cαs of V478 was taken as the zero position.
A potassium ion was restrained with a harmonic potential with a coefficient of 1,000 kJ/mol(nm)^2.
Three sets of the sampling simulations were run. For each set, the center of the harmonic potential well was moved at 0.1nm intervals from -0.8nm ~ +1.7nm.
During the sampling, only the peptide backbone atoms were harmonically restrained with the coefficient of 1,000kJ/mol(nm)^2, while the amino acid sidechain atoms were not restrained. (We also carried out several sets of umbrella sampling analyses without restraining the peptide backbone, and obtained similar results; the S6 structure remained largely unchanged for the 100ps period during which the umbrella sampling was performed.)
Since the surface hydration of the ion conduction pathway is critical in the free energy analysis and any difference in the degree of hydration appears to complicate the results, in the current study we chose to re-fill the ion conduction pore (including the central cavity) with water and perform a 100ps pre-run before the umbrella sampling. These water molecules were not restrained and no external electric field was applied. From the sampling data, a histogram (100 bins covering the z-position of -1.2nm to +1.8nm) was obtained and the analysed with the weighted histogram analysis method, or WHAM (48).
The program gmx-wham.c of the Gromacs suit (contributed by Dr. David Bostick) was used with a minor modification.

..

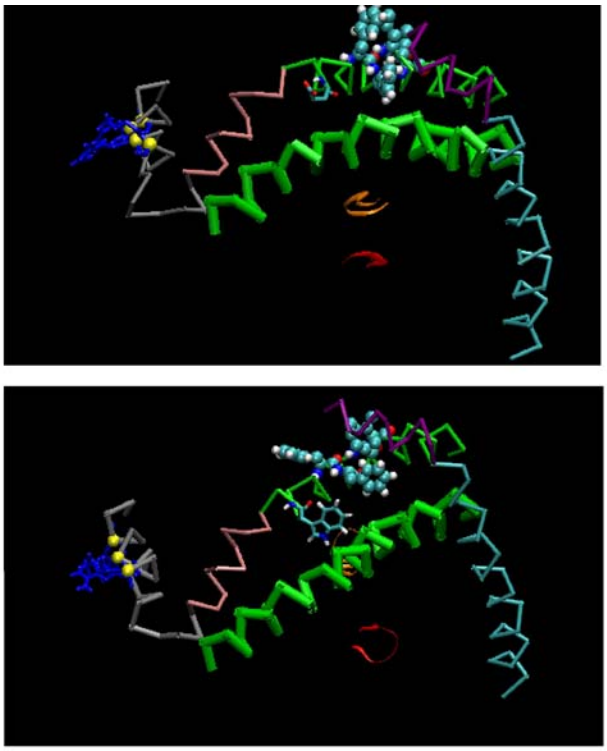

Fig.S5 Effect of E395W on S6 conformation.
Top: wt-chimera-Eo-S4middle viewed from the bottom at 12ns.
Thin and thick green trances show S5 and S6, respectively.
For S5, E395 is shown in licorice, whereas F401 and F402 are
shown in the van del Waals representation.
Orange and red ribbons represent two opposing loops forming the selectivity filter.
S4 is shown as a silver trace and the gating-charge-carrying arginine residues
are shown in blue licorice.
Bottom: E395W-Eo-S4middle viewed from the bottom at 12ns.
The same representation scheme is used as in the top figure.
Note that E395W appears to push S6 toward the central axis of the pore domain.

Comment on the effect of F401A and F402A.
S4 with F401A-F402A may partially lose its ability to pull up
the adjacent subunit S5, causing the pore domain to remain
in the closed state (G-V relation positively shift).
Alternatively, F401A and F402A may render the hydrophobic interaction
so weak that the z-position of the S4-S5 linker becomes too low
for the given position of the adjacent subunit S5.

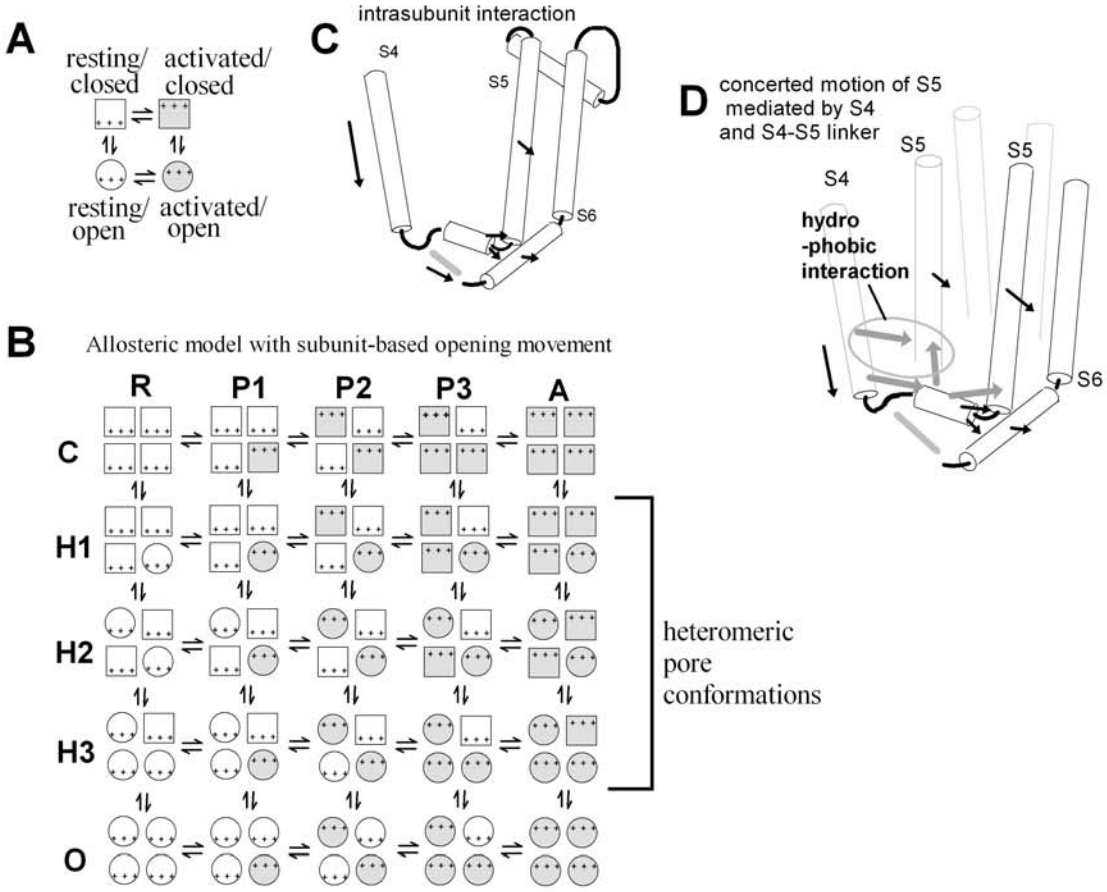

Fig.S6 Proposed model for the conformational change associated with the transition from the open/activated state to the closed/resting state.
(A) The simplest representation of the allosteric model. Voltage sensor movement (resting and activated states are represented by white and gray, respectively) is allosterically coupled to the channel opening (closed vs. open, represented by squares and circles respectively).
(B) The general allosteric model for a protein with four subunits and two distinct conformational changes shown in (A). Note that this model allows heteromeric pore opening. This representation is basically the same as the one shown in Chapman et al. (62). Symbols used are the same as in (A). (C) A model for mechanical coupling between S4 (and the S4-S5 linker) and S6 as a basis of subunit-based movement.
(D) Proposed model for the mechanical coupling of how the S4 downward translocation leads to concerted motion of S5 in two subunits. S4 is hypothesized to pull down S5 of the adjacent subunit in two ways as shown by two straight gray arrows: via direct interaction and via the interaction between the S4-S5 linker and the S5. S4 is also likely to pull down S5 of the same subunit as shown in (C). This explains why two out of four subunits exhibit greater S5 movement when S4 of just one of the subunits is pulled down (see text). Direct interaction between S5 and S5 of different subunits appears to be insignificant and is not shown in this figure.

Comment on the Hill analysis of Kv channel.
Kv channel's Hill coefficient was slightly greater than 1, indicating a small degree of between-subunit cooperativity (26). However, the process can be taken into account by the Hill analysis only when the process is associated with energy change such as chemical, potential or conformational energy. Of note, the conformational change of the Kv channel voltage sensor is associated with a large amount of free energy due to the gating charge, but S5 and S6 movement shows little voltage dependency and is associated with relatively small free energy differences. Consequently, while the Hill analysis should place a large weight on S4 movements, it places only a small weight on movement of the pore domain.